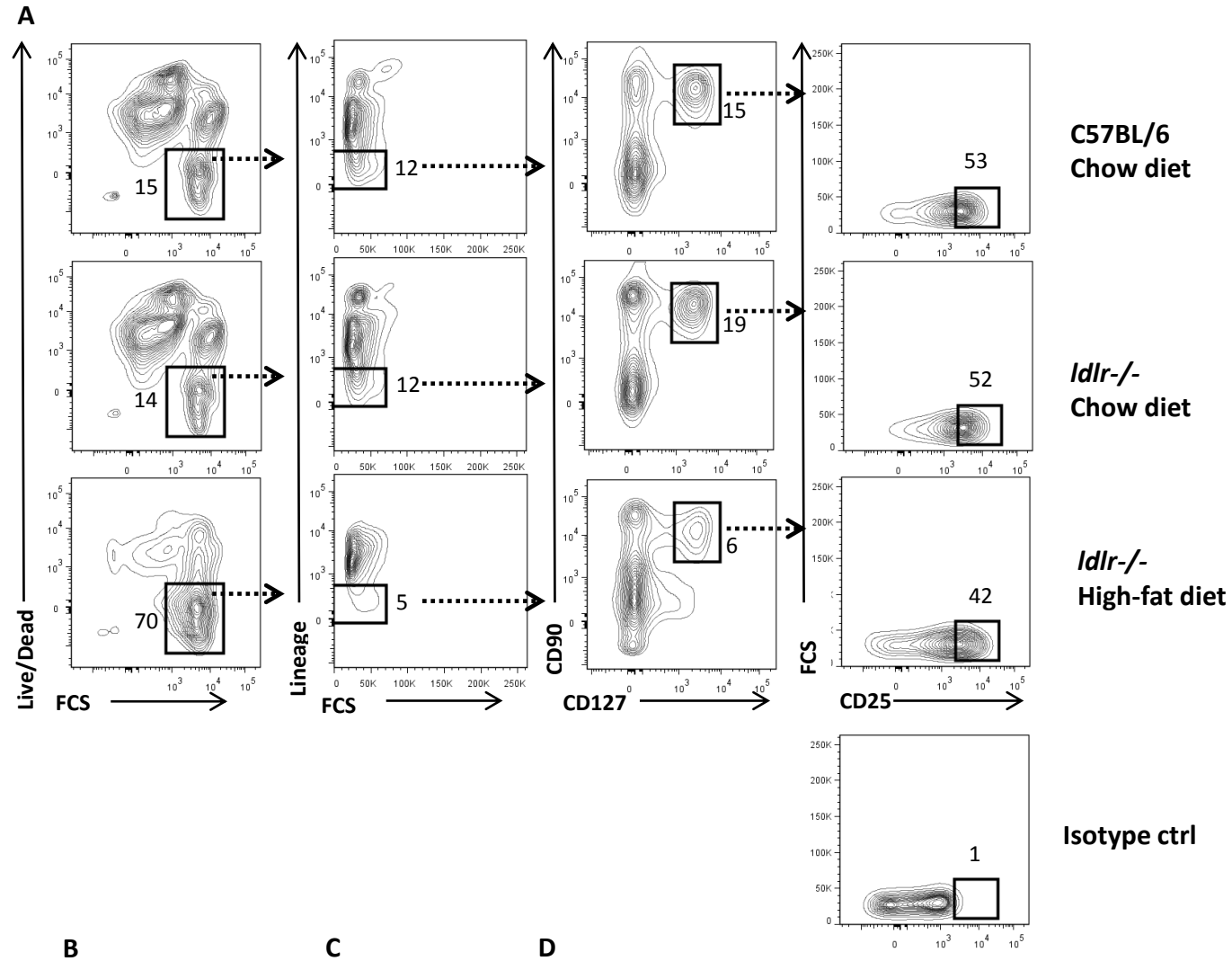

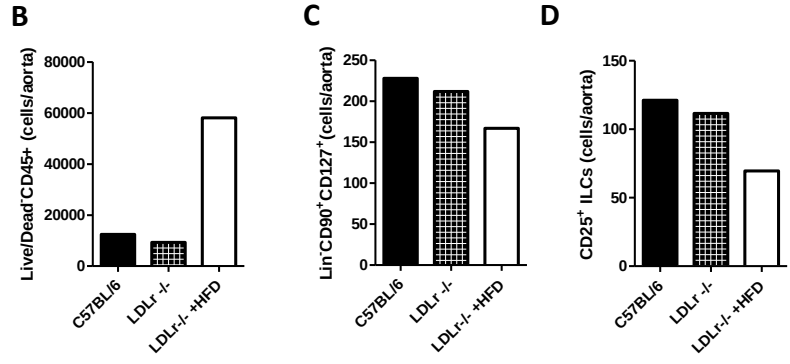

Supplemental Figure I. High-fat diet feeding does not influence levels of ILCs in the aorta
(A)Gating strategy of $CD45^+$lineage (lin)$^-CD90^+CD127^+CD25^+$ ILCs in digested aorta. Isotype control anti-CD25.
(B)Number of $CD45^+$ leukocytes, (C) $lin^-CD90^+CD127^+$ ILCs or (D) $lin\text{-}CD90^+CD127^+CD25^+$ ILCs per aorta. n=5 mice/pool.

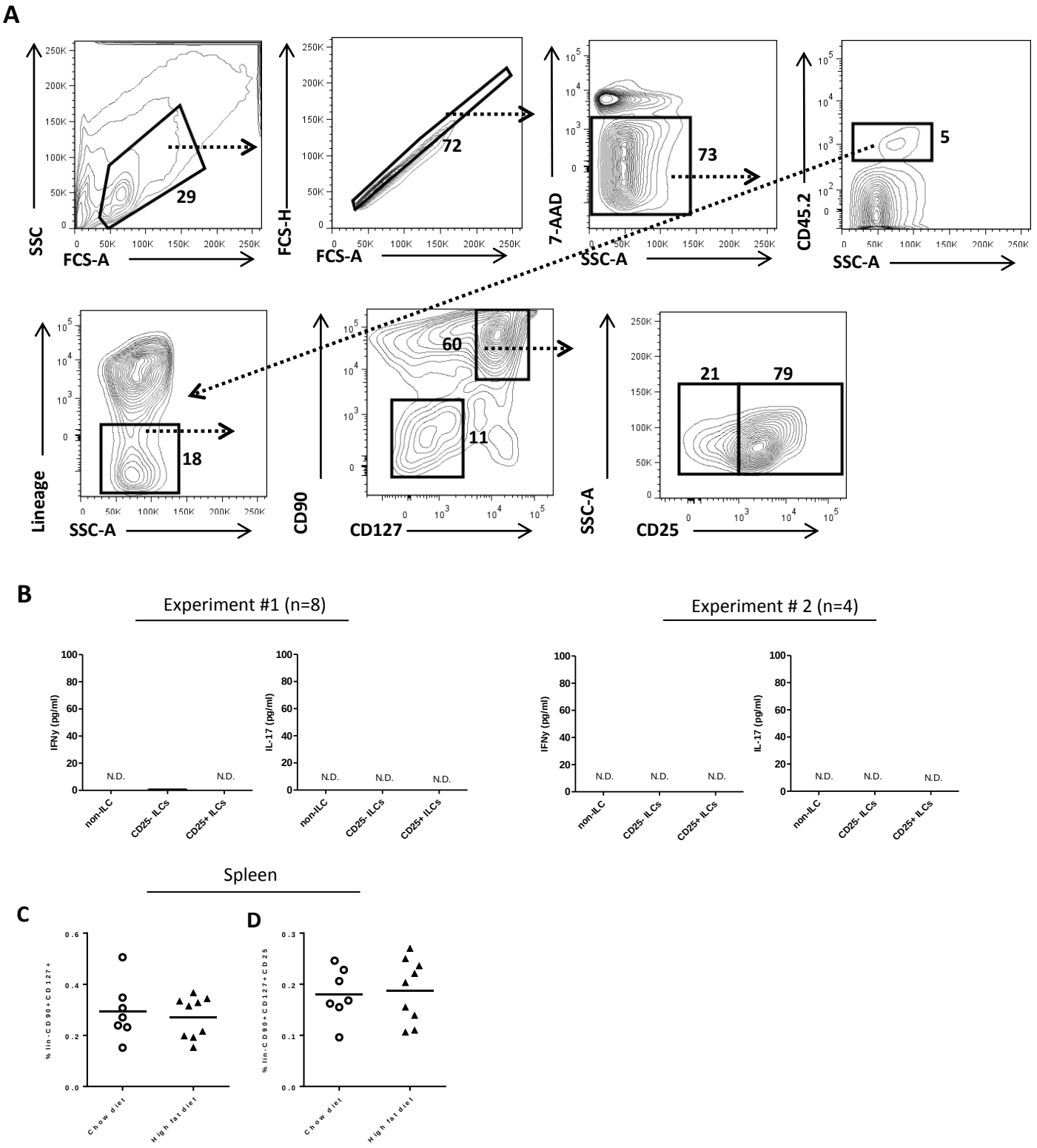

Supplemental Figure II. Gating strategy for aortic CD90$^+$CD127$^+$CD25$^+$ ILCs from *rag1-/-ldlr-/-* mice.
(A) Gating strategy for identification of aortic ILCs.
(B) Aortic lin$^-$CD90$^-$CD127$^-$ (non-ILCs), CD25- ILCs and CD25$^+$ ILCs sorted by FACS and stimulated with PMA/ionomycin. Levels of IFNγ and IL-17 in supernatants from stimulated cells was measured in two separate experiments. (C) Quantification of splenic ILCs in *rag1-/-ldlr-/-* mice fed chow or high-fat diet (n=7-9).

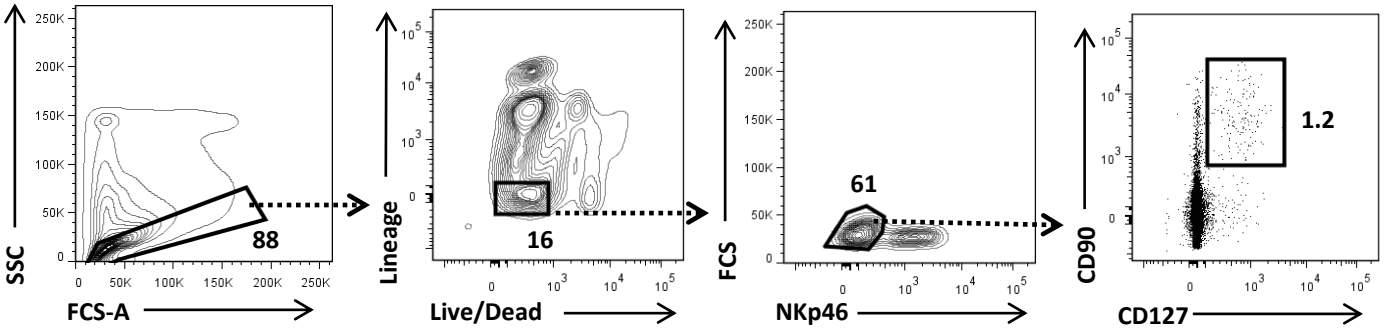

Supplemental Figure III. Gating strategy for identification of splenic lineage- CD90^{+}CD127^{+} ILCs.
Representative gating of splenic lin^{-}CD90^{+}CD127^{+} ILCs from a *rag1-/-ldlr-/-* mouse fed high-fat diet and treated with control IgG..

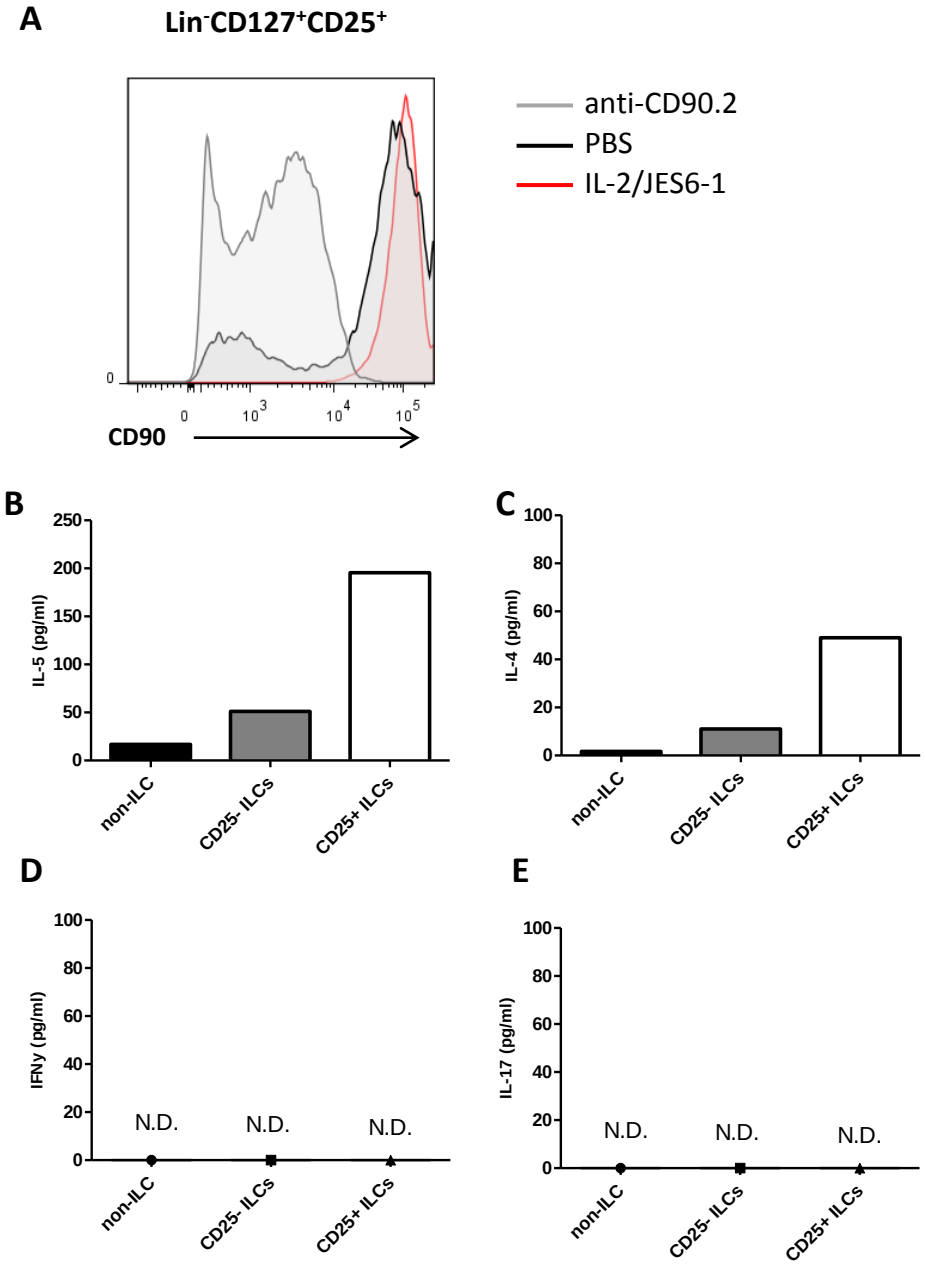

Supplemental Figure IV. Aortic ILCs from anti-CD90.2 injected mice produce type 2 cytokines.
(A) Expression of CD90 on aortic lin$^-$CD127$^+$CD25$^+$ cells from anti-CD90.2 injected *rag1-/-ldlr-/-* mice. ILCs (CD25$^+$ or CD25$^-$) or non-ILCs were sorted from anti-CD90.2 treated mice and stimulated with PMA/ionomycin for 24h. (B)IL-5, (C) IL-4, (D) IFNγ and (E) IL-17 was measured in the supernatant.

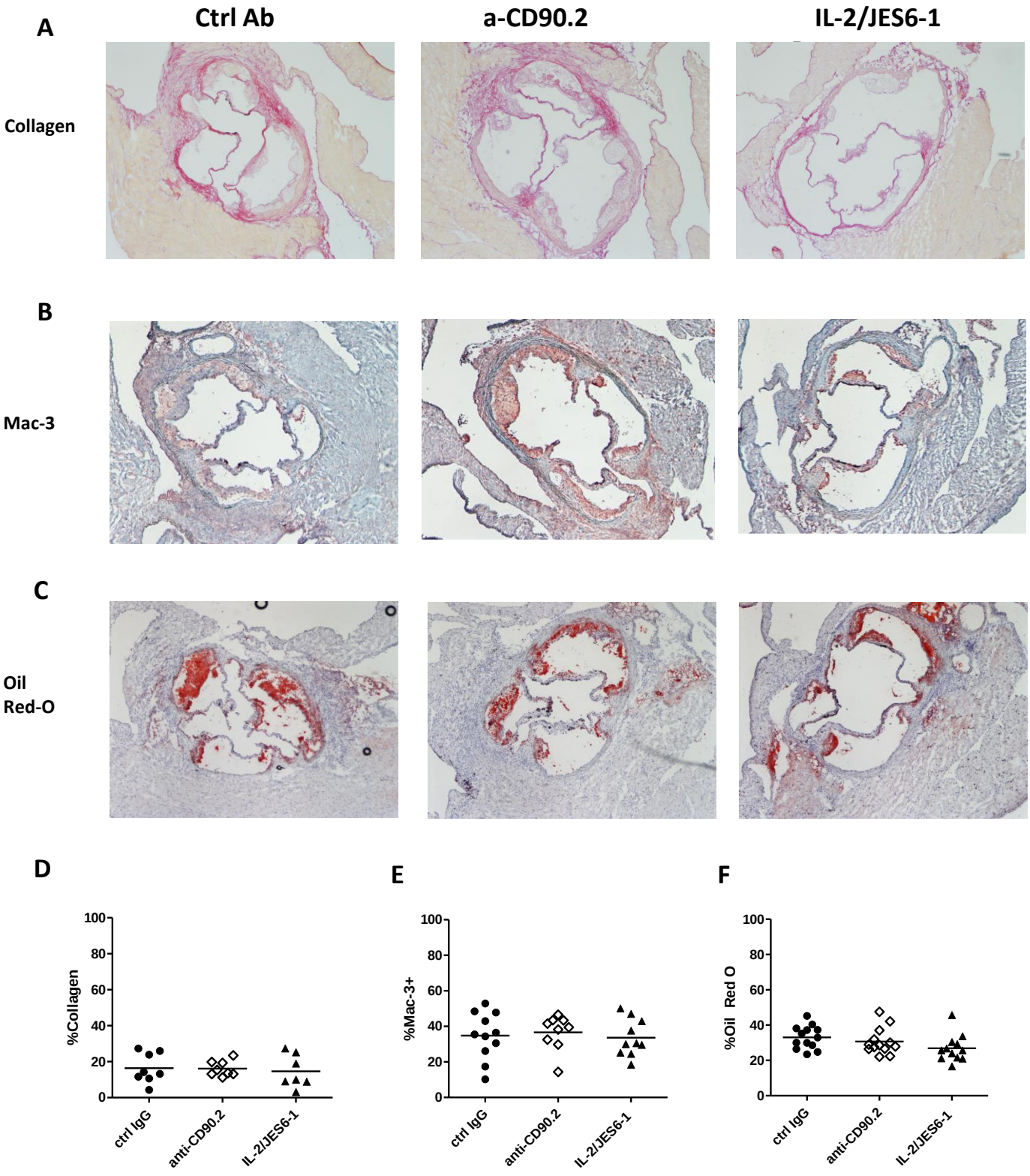

Supplemental Figure V. No effect of ILC depletion or expansion on lesion composition
(A) Collagen (Van Gieson), (B) macrophage (Mac-3) and (C) Oil Red-O staining of aortic sinus. Quantification of (D) Collagen, (E) macrophages and (F) Oil Red O comparing treatment groups (n=8-10).

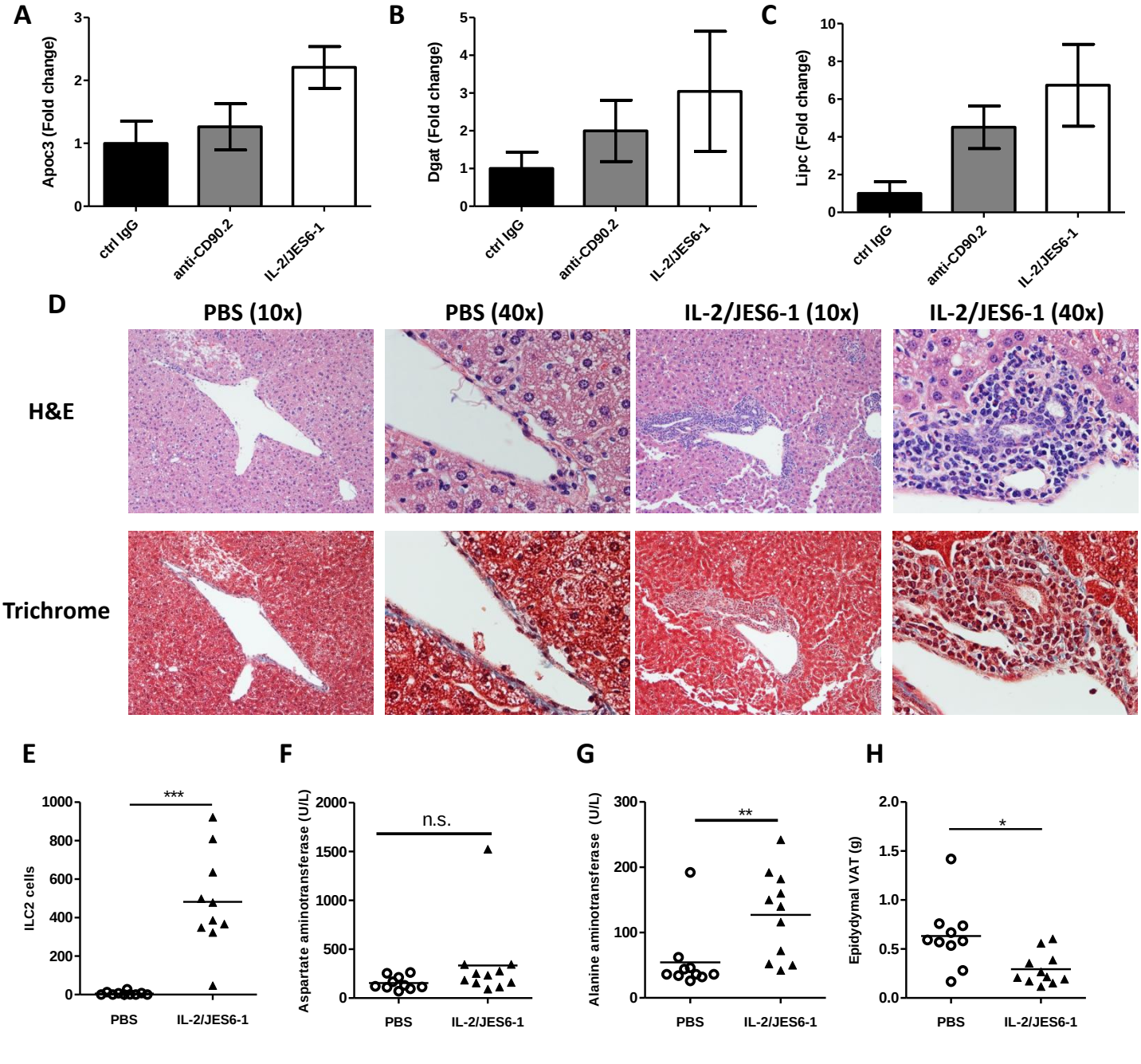

Supplemental Figure VI. Effects of CD25+ ILC expansion on liver and adipose tissue.

Hepatic RNA was isolated from mice treated with control IgG, anti-CD90.2 or IL-2/JES6-1. (A) mRNA expression of apolipoprotein C-III (Apoc3), (B) diglyceride acetyltransferase (Dgat), and (C) hepatic lipase (Lipc) was measured by qRT-PCR (n=7-11. Mean± SEM).

In a follow–up experiment, mice were fed HFD for seven weeks and treated with PBS or IL-2/JES6-1 for the last four weeks. (D) Representative liver sections from *rag1*$^{-/-}$*ldlr*$^{-/-}$ mice stained with H&E or Masson's Trichrome stain (magnification 10x and 40x).

(E) Levels of aspartate aminotransferase and (F) alanine aminotransferase were measured in serum. (G) Epididymal visceral adipose tissue and (H) liver resident ILC2s (lin^{-}CD90^{+}CD25^{+}ST2^{+})after seven weeks of high-fat diet and IL-2/JES6-1 treatment. (n=10-11)

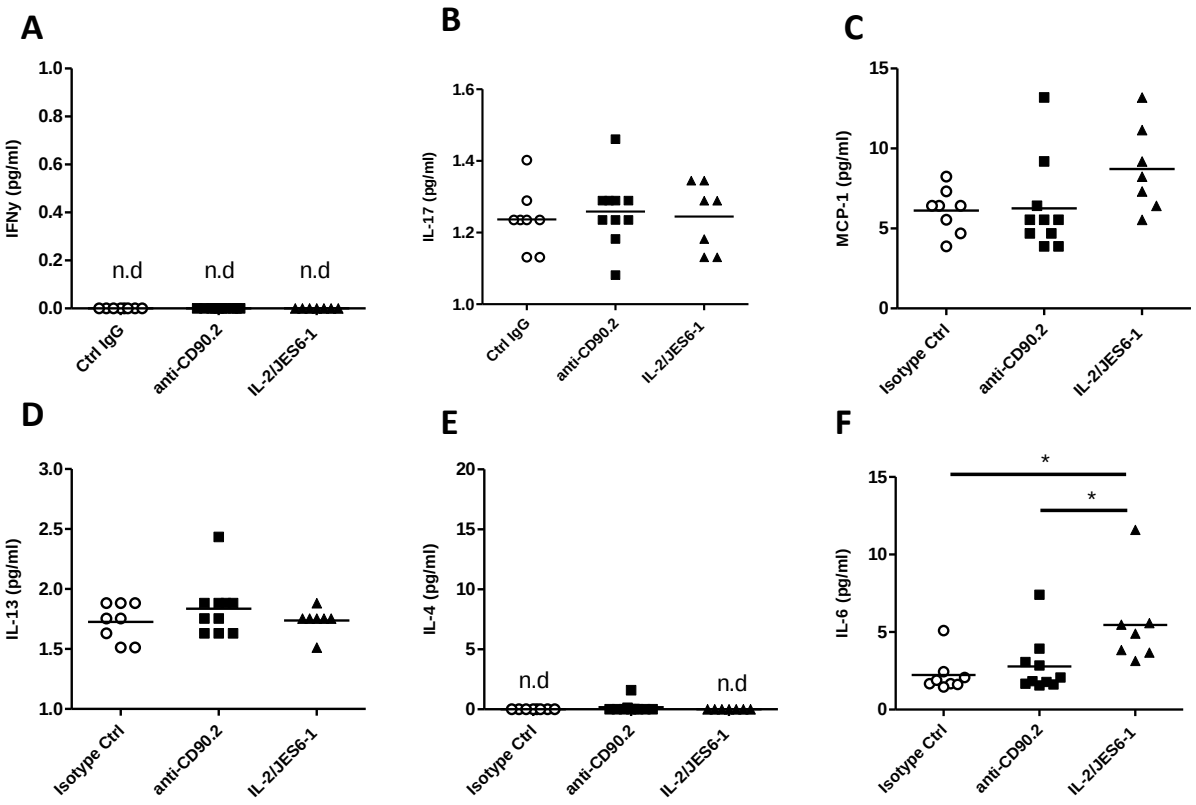

Supplemental Figure VII. Levels of serum cytokines in ILC depleted or IL-2/JES6-1 treated mice
Serum levels of (A) IFNy, (B) IL-17, (C) MCP-1, (D) IL-13, (E) IL-4, (F) IL-6 comparing control IgG, anti-CD90.2 and IL-2/JES6-1 treated *rag1-/-ldlr-/-* mice. (n= 7-10).

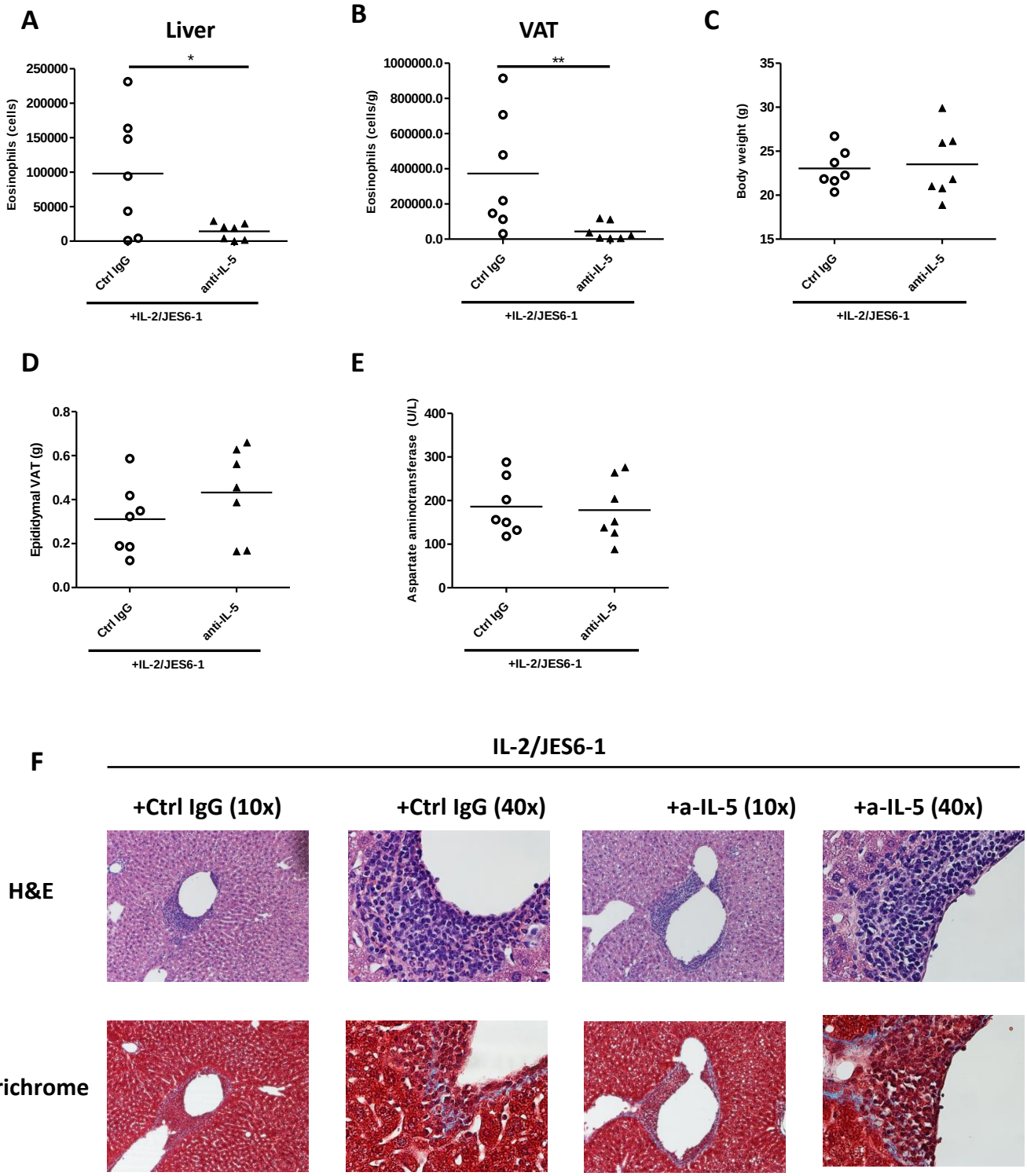

Supplemental Figure VIII. Liver inflammation and fibrosis by IL-2 complex treatment is independent of IL-5
(A) Quantification of eosinophil accumulation to (A) liver and (B) epididymal VAT of mice treated with IL-2 complex combined with either anti-IL-5 or control IgG (ctrl IgG). (C) Body weight, (D) epididymal VAT and serum levels of (E) aspartate aminotransferase. (F) Liver sections stained with H&E or Masson's trichrome (10x and 40x magnification). n=7/group.